Material Flow around a Bobbin Tool for Friction Stir Welding

J. Hilgert[*,1], L.L. Huetsch[1,] J.F. dos Santos[1] and N. Huber[1]
[1]GKSS Forschungszentrum, Institute of Materials Research, Materials Mechanics, Solid-State Joining Processes (WMP), Geesthacht, Germany
*Corresponding author: Max-Planck-Straße 1 - 21502 Geesthacht - Germany, Jakob.hilgert@gkss.de

Abstract: This study presents an approach to model the material flow around a bobbin tool for Friction Stir Welding (FSW). In this CFD model the aluminum is treated as a highly viscous non Newtonian shear thinning liquid.
The model is formulated in a 3D Eulerian frame. The temperature field and the desired torque acting on the tool are taken from a 3D thermal pseudo mechanical model implemented in Comsol and Matlab that was presented at last years Comsol Conference in Milano. The results of the CFD model provide the material flow field, the amount of sticking and slipping at the interface between tool and plates as well as the forces acting on the tool.
Experiments on the "FlexiStir" experimental welding unit have been carried out to successfully validate the torque assumptions and the shear layer shape for welds of aluminum alloy AA2024-T3 4mm sheets.

Keywords: FSW, Bobbin Tool, CFD

1. Introduction

Friction stir welding was developed and patented by Wayne Thomas [1]. It is a solid state joining process capable of welding a great number of materials. These include Al, Pb, Mg, Ti, Cu, Zn, steels [2,3] and especially hard to weld alloys [4-6] including ODS Aluminum alloys [7].
The process is carried out by plunging a rotating tool into the material and translating it along the weld line. The heat generated by friction at the tool surface and plastic dissipation soften the material to a plasticized state. The material is then sheared around the tool and forms a weld. The conventional tool design consists of a shoulder and a pin. A second class of tools, called bobbin tools, includes a second shoulder attached to the end of the pin (see fig. 1).

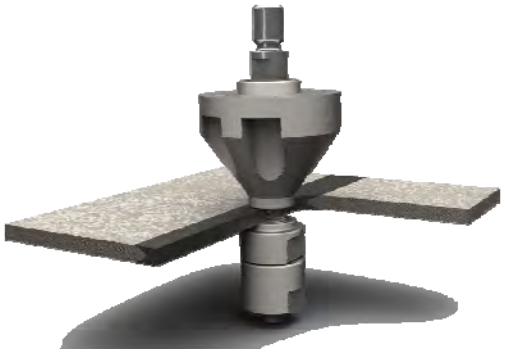

Figure 1. Overview of the FSW process using a bobbin tool.

These tools have some advantages over conventional tools. They do not require an applied plunging force in vertical direction as the loads are carried within the pin. Therefore closed profiles that do not allow for a backing bar can be welded with this process. The challenge in using bobbin tools is the high load on the pin. This load is hard to determine experimentally even with instrumented tools (compare [8]). The pressure distribution needs to be known for tool design and selection of welding parameters. In order to understand the formation of a sound weld the material flow in the shear layer around the tool also needs to be known. Both can be found using numerical simulation.
To the Authors best knowledge there is no report in literature yet on the flow around a bobbin tool. Promising work has recently been published on the material flow around conventional FSW tools [9-16].
It is possible to extend existing modeling attempts to two shoulder configurations. The focus is not the same when it comes to desired results, though. Because of the great importance for bobbin tools development the present work focuses on the loads on the pin.
For the optimization of process parameters a great number of solutions for different process parameters are needed. Therefore this model is designed for high performance rather than high detail.

The complete details of the study described here are submitted for publication in “Welding In the World”.

2. Model

2.1 Thermal Data

The temperature data used in this study are taken from a thermal model using an iterative mapping technique called Moving Geometry modeling. It was presented at last years Comsol Conference in Milano and is described in detail in [17]. The model captures the motion of the bobbin tool along the weld line in a Lagrangian frame. It uses only thermal degrees of freedom.
A unique capability of the TPM heat source used in that model is to predict the machine torque from a numerical simulation with only thermal degrees of freedom. This is done by integrating the temperature dependent material flow stress multiplied with the distance from the rotational axis of the tool over the contact surface of the tool and the work piece.

2.2 Flow Model

A CFD model is set up in Comsol. The geometry (see fig. 2) consists of a section of the base material sheets and the tool pin. The tool shoulders are imprinted as boundaries on the top and bottom surface of the work piece.
The mesh consists of about 85000 second order tetrahedron elements adding up to about 375000 degrees of freedom.
The governing equation is the Navier-Stokes equation (eq. 1)

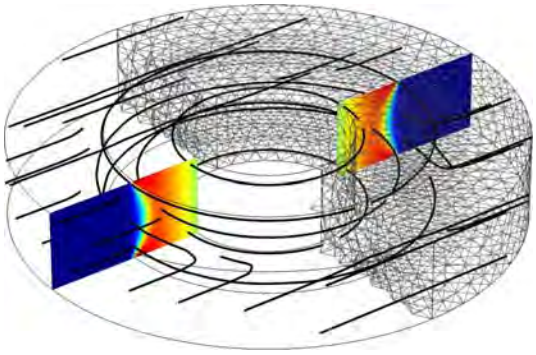

Figure 2. Geometry and mesh of the flow Model. Streamlines and colored slice data show an example of a velocity field solution.

$$\begin{aligned} \rho(u\cdot\nabla)u &= \nabla\cdot[-pI+\eta(\nabla u+(\nabla u)^T)] \\ \nabla\cdot u &= 0 \end{aligned}$$

Equation 1

The viscosity is defined using the inverse hyperbolic sine law [18]. It is a function of temperature and shear rate. The standard form in terms of effective deviatoric flow stress $\bar{\sigma}$ and effective strain rate $\dot{\bar{\varepsilon}}$ is given in (eq. 2). In terms of effective viscosity η_{eff} and shear rate $\dot{\gamma}$ this yields (eq. 3).

$$\bar{\sigma} = \frac{1}{\alpha} sinh^{-1}\left(\frac{\dot{\bar{\epsilon}} e^{(Q/(RT))}}{A}\right)^{1/n}$$

Equation 2

$$\eta_{eff} = \frac{sinh^{-1}\left(\frac{\dot{\gamma} e^{(Q/(RT))}}{\sqrt{3}A}\right)^{1/n}}{\alpha\dot{\gamma}\sqrt{3}}$$

Equation 3

Here R is the universal gas constant and α, A, Q, and n are material properties. For the alloy AA2024 these constants are taken from [19] and given in (table 1).

Table 1: Material Parameters for AA2024

α	1.6e-8 [m^2/N]
A	$e^{19.6}$ [s^{-1}]
Q	1.4880e5 [J/Mol]
n	4.27

As the viscosity is described by a very nonlinear function a parametric solver approach is needed to achieve convergence. Hereby the effective viscosity is ramped up using a convergence parameter n_{conv} going from 10 to 1 according to (eq. 4).

$$\eta_{conv} = \eta_{eff}(\dot{\gamma}, T)^{(1/n_{conv})}$$

Equation 3

The boundary conditions of the inlet and outlet surface define a constant material flow velocity

in welding direction. This represents the actual behavior of the material, which does not deform outside a small shear layer around the tool. The free surface of the plate is set to have slip condition so that no material can leave the plate. The pin and shoulder surfaces prescribe a defined tangential velocity $v_{tangent}$ compatible with the tools rotation speed ω according to (eq. 5).

$$v_{tangent} = \delta \omega r$$

Equation 5

Here r is the distance from the tool axis, ω is the tools angular velocity and δ is the contact state variable ($0<\delta<1$) that defines the ratio of sticking and slipping at the interface.

The torque M_T acting in the pin can be calculated according to (eq. 6).

$$M_T = \int_{\partial\Omega} (Fv_x \cdot y - Fv_y \cdot x) dA$$

Equation 6

Where Fv is the viscous force per area acting on a location on the pin surface and x and y are the distances from the tool axis.

A global constraint can be applied to the torque variable defining a constant value known from the thermal model and validated experimentally. The global Temperature field is taken from the same source. This way the contact state variable δ can be determined. As an alternative the desired contact state can be prescribed and the torque can be predicted from the CFD model.

The steady state solution of one set of process parameters (welding speed, rpm) takes about one minute on a state of the art workstation featuring two quad core Intel Xeon Processors @ 2.93GHz and 32GB of RAM.

Transient predictions can be made (see [16]). The computational effort scales linearly with the amount of time steps. The duration of one time step should be chosen such that the translation of the tool is no larger than one fifth of the shoulder diameter. One hundred steps are usually sufficient for a transient model of a run-in or run-out.

3. Experimental Validation

The shape and size of the predicted shear layer as well as the torque M_T which is predicted by the thermal and used by the CFD model, are validated experimentally. The Material used is a sheet of AA2024 in T351 condition. It is welded using a bobbin tool with a 8mm pin and 15mm scrolled shoulders similar to those shown in (fig. 1). The process parameters welding speed $u_{weld} = 1mm/s$ and tool rotation rpm = 1000 are used. While welding the machine torque is monitored using the spindle motor current. After welding a sample is taken from the weld, then polished and etched with Keller's solution to reveal the shear layer shape.

An example of a shear layer velocity profile predicted with the CFD model is compared to the macrograph of an experimental weld in (fig. 3).

The torque measured during the experiment is subject to a large amount of scatter. Evaluating a time of 4s with a sampling rate of 100Hz a mean value of 14.1Nm with a standard deviation of 0.7Nm are found ~5%). When running in idle mode the torque due to losses in motors and bearings is 4.1Nm with a standard deviation of 0.6Nm. This means that the controlling source of scatter is the idle torque. The mean measured welding torque M_T is 10.0Nm. It can readily be assumed that the scatter of this value is far below 5%. This is in very good agreement with the steady state value of 9.9Nm predicted by the TPM thermal model.

The prediction shows good agreement in shear layer shape. The absolute value of the predicted shear layer velocity is not easy to validate experimentally. New experiments based on marker material investigation need to be developed.

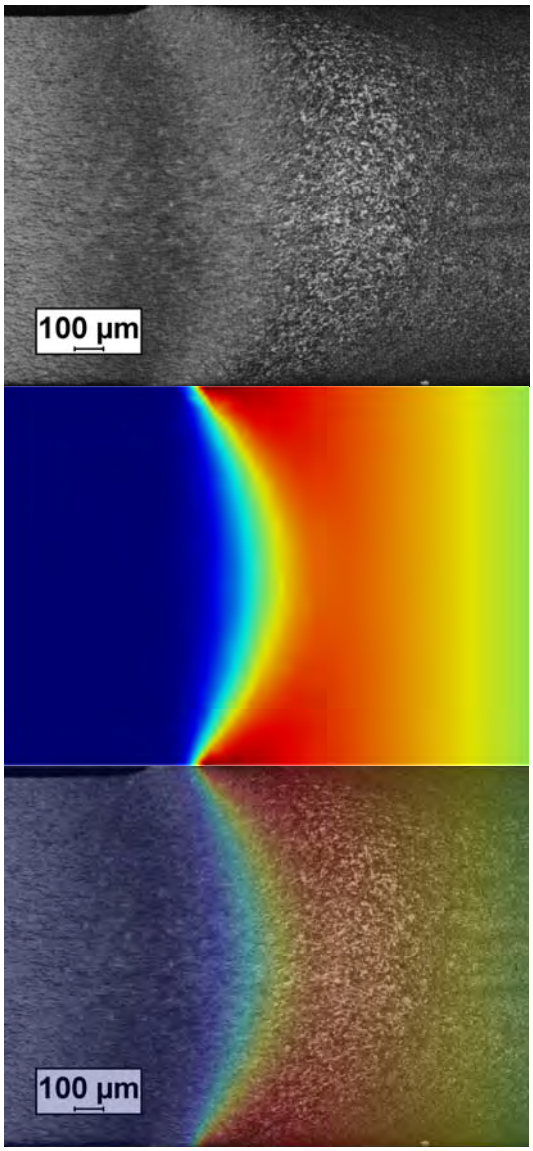

Figure 3. Comparison between a predicted shear layer and a macrograph of the resulting microstructure of a weld. Red color indicates high velocity.

4. Force Predictions

The model predictions include the viscous force per area Fv distribution on the pin and shoulders.

When integrating the viscous force per area on all tool boundaries the resulting forces Fw in welding and Fl in the lateral direction can be evaluated for pin and shoulders.

Figure 4 plots the resulting total force as a function of welding speed and tool rotation speed.

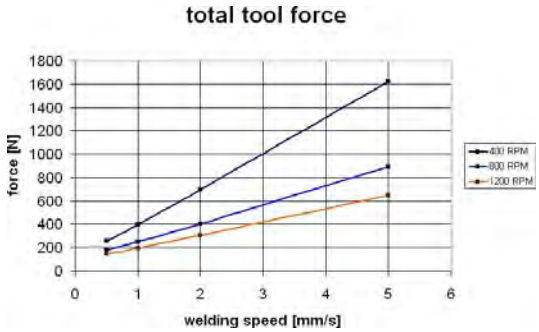

Figure 3. Resulting total force on the tool as a function of welding speed and tool rotation speed.

5. Conclusions

The shear layer shape around FSW bobbin tools can be predicted using Comsol Multiphysics[tm]. The resulting shear layer shape is in good agreement with experimental evidence. The resulting forces on the tool can be predicted. When treating Aluminum as shear thinning liquid the highly nonlinear material model calls for a convergence parameter.

6. References

1. Thomas, W.; Nicholas, E.; Needham, J.; Murch, M.; Templesmith, P. & Dawes, C. *Friction stir welding Patent Application No. PCT/GB92102203 and Great Britain Patent Application No. 9125978.8*, (1991)

2. Uyyuru, R. & Kailas, S., Numerical Analysis of Friction Stir Welding Process, *Journal of Materials Engineering and Performance*, **15**, 505-518 (2006)

3. Thomas, W.; Johnson, K. & Wiesner, C., Friction Stir Welding - Recent Developments in Tool and Process Technologies, *Advanced Engineering Materials*, **5**, 5867-5877 (2003)

4. Zhang, Z., Comparison of two contact models in the simulation of friction stir welding process, *J Mater Sci*, **43**, 5867-5877 *(*2008)

5. Su, J.-Q.; Nelson, T.; Mishra, R. & Mahoney, M., Microstructural investigation of friction stir welded 7050-T651 aluminium, *Acta Materialia*, , **51,** 713-729 (2003)

6 Cook, G.; Crawford, R.; Clark, D. & Strauss, A., Prediction of temperature distribution and thermal history during friction stir welding: input torque based model, *Industrial Robot: An International Journal*, **31**, 55-63 *(*2004)

7. Cavaliere, P.; Cerri, E.; Marzoli, L. & dos Santos, J., Friction Stir Welding of Ceramic Particle Reinforced Aluminium Based Metal Matrix Composites, *Applied Composite Materials*, **11**, 247-258 (2004)

8. Hattingh, D.; Blignault, C.; van Niekerk, T. & James, M., Characterization of the influences of FSW tool geometry on welding forces and weld tensile strength using an instrumented tool, *Journal of Materials Processing Technology*, **203**, 46 - 57 (2008)

9. Xu, S.; deng, X.; Reynolds, A. & Seidel, T. Finite element simulation of material flow in friction stir welding *Science and Technology of Welding & Joining*, **6**, 191-193 (2001)

10. Dong, P.; Lu, F.; Hong, J. & Cao, Z., Coupled thermomechanical analysis of friction stir welding process using simplified models, *Science and Technology of Welding & Joining*, **6**, 281-287 (2001)

11. Seidel, T. & Reynolds, A., Two-dimensional friction stir welding process model based on fluid mechanics, *Science and Technology of Welding & Joining*, **8**, 175-183 (2003)

12. Colegrove, P. & Shercliff, H., Two-dimensional CFD modelling of flow round profiled FSW tooling, *Science and Technology of Welding & Joining*, **9**, 483-492 (2004)

13. Schmidt, H. & Hattel, J., A local model for the thermomechanical conditions in friction stir welding, *Modelling Simul. Mater. Sci. Eng.*, **13**, 77-93 (2005)

14. Colegrove, P. & Shercliff, H., CFD modelling of friction stir welding of thick plate 7449 aluminium alloy, *Science and Technology of Welding & Joining*, **11**, 429-441(13) (2006)

15. Zhang, H.; Zhang, Z. & Chen, J., 3D modeling of material flow in friction stir welding under different process parameters, *Journal of Materials Processing Technology*, **183**, 62-70 (2007)

16. Schmidt, H. & Hattel, J., Thermal and Material Flow modelling of Friction Stir Welding using Comsol, *Proceedings of the COMSOL Conference 2008 Hannover*, (2008)

17. Hilgert, J.; Schmidt, H.; dos Santos, J. & Huber, N., Thermal Models for Bobbin Tool Friction Stir Welding, *accepted by Journal of Materials Processing Technology*, (2010)

18. Aukrust, T. & LaZghab, S., Thin shear boundary layers in flow of hot aluminium, *International Journal of Plasticity*, **16**, 59 - 71 (2000)

19. Sheppard, T., Extrusion of AA 2024 alloy, *Materials Science and Technology*, **9**, 430-440(11) (1993)

7. Acknowledgements

This work was kindly supported by GKSS Forschungszentrum GmbH, Institute of Materials Research, Materials Mechanics and Joining, Solid-State Joining Processes (WMP), Geesthacht, Germany.